

# SubEdit: A Representation for Editing Measured Heterogeneous Subsurface Scattering

Ying Song \* †

Xin Tong †

Fabio Pellacini ‡

Pieter Peers §

Zhejiang University\*  
State Key Lab. of CAD&CG

Microsoft Research Asia†

Dartmouth College‡  
University of Southern California§  
Institute for Creative Technologies

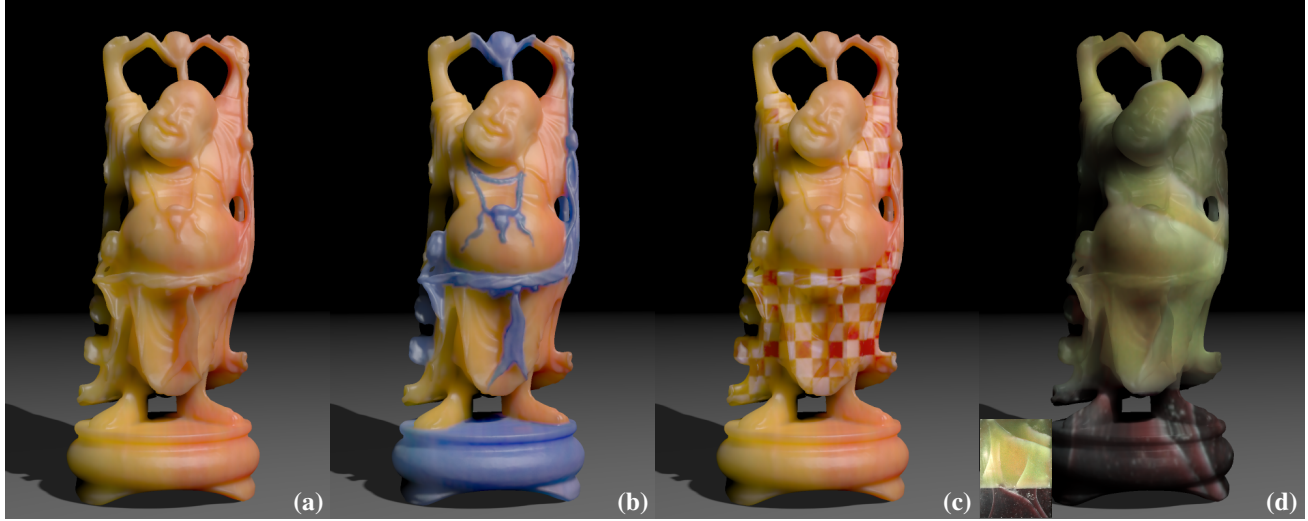


**Figure 1:** Different edited versions of a measured heterogeneous yellow wax material applied to the Buddha model. (a) A rendering of the original material applied to the model. (b) Material painting: a different measured blue wax material is painted over selected parts of the Buddha model. The interface between both materials is automatically handled by SubEdit. (c) Pattern copy-and-paste: a pattern is copied from a measured chessboard dataset and pasted on the yellow wax. (d) BSSRDF hallucination: a BSSRDF is generated from just a single photograph of the target material (inset) using the yellow wax material as a guide.

## Abstract

In this paper we present *SubEdit*, a representation for editing the BSSRDF of heterogeneous subsurface scattering acquired from real-world samples. Directly editing measured raw data is difficult due to the non-local impact of heterogeneous subsurface scattering on the appearance. Our *SubEdit* representation decouples these non-local effects into the product of two local scattering profiles defined at respectively the incident and outgoing surface locations. This allows users to directly manipulate the appearance of single surface locations and to robustly make selections. To further facilitate editing, we reparameterize the scattering profiles into the local appearance concepts of albedo, scattering range, and profile shape. Our method preserves the visual quality of the measured material after editing by maintaining the consistency of subsurface transport for all edits. *SubEdit* fits measured data well while remaining efficient enough to support interactive rendering and manipulation. We illustrate the suitability of *SubEdit* as a representation for editing by applying various complex modifications on a wide variety of measured heterogeneous subsurface scattering materials.

## 1 Introduction

Many real world materials such as wax, marble, and skin exhibit light scattering within the object volume. This subsurface scattering significantly impacts the visual appearance of these translucent objects. Heterogeneous subsurface scattering, as opposed to homogeneous subsurface scattering, is the result of the complex spatial variations of the scattering properties of the medium together with the structural deficiencies and impurities found inside the object (e.g., the veins in marble). The complex interactions of all these parameters makes the modeling of realistic heterogeneous subsurface scattering materials difficult. Often, the acquisition of real world samples is the most straightforward way to obtain realistic models. In recent years several methods have been developed to efficiently acquire and compactly represent subsurface scattering appearance [Goesele et al. 2004; Chen et al. 2004; Tong et al. 2005; Wang et al. 2005; Peers et al. 2006]. The focus of these representations is to efficiently reproduce and render an exact copy of the measured appearance, without explicitly considering its modification. For many applications though, such as cinematic rendering and fine arts, artistic editing of measured materials is necessary. This is the focus of our work.

Subsurface scattering can be described by the *bidirectional subsurface scattering reflectance distribution function* (BSSRDF) that expresses the light transport between pairs of surface points [Nicoletti et al. 1977]. The BSSRDF directly encodes surface appearance induced by the complex light transport interactions within the object’s volume. This non-local influence on the appearance of a specific surface point poses specific challenges in editing a measured heterogeneous BSSRDF that are absent in many other appearance editing systems (e.g., [Lawrence et al. 2006; Pellacini

### ACM Reference Format

Song, Y., Tong, X., Pellacini, F., Peers, P. 2009. SubEdit: A Representation for Editing Measured Heterogeneous Subsurface Scattering. *ACM Trans. Graph.* 28, 3, Article 31 (August 2009), 10 pages.  
DOI = 10.1145/1531326.1531337 <http://doi.acm.org/10.1145/1531326.1531337>.

### Copyright Notice

Permission to make digital or hard copies of part or all of this work for personal or classroom use is granted without fee provided that copies are not made or distributed for profit or direct commercial advantage and that copies show this notice on the first page or initial screen of a display along with the full citation. Copyrights for components of this work owned by others than ACM must be honored. Abstracting with credit is permitted. To copy otherwise, to republish, to post on servers, to redistribute to lists, or to use any component of this work in other works requires prior specific permission and/or a fee. Permissions may be requested from Publications Dept., ACM, Inc., 2 Penn Plaza, Suite 701, New York, NY 10121-0701, fax +1 (212) 869-0481, or permissions@acm.org.  
© 2009 ACM 0730-0301/2009/03-ART31 \$10.00 DOI 10.1145/1531326.1531337  
<http://doi.acm.org/10.1145/1531326.1531337>

and Lawrence 2007]). On the one hand, it is difficult for users to *directly manipulate the appearance of single surface locations* without some "decoupling" of the non-local effects of subsurface scattering. On the other hand, the non-local *consistency of the BSSRDF* function itself should be maintained while editing to avoid rendering artifacts, a complex task when directly manipulating the raw measured BSSRDF data. While directly editing the underlying volumetric material properties would certainly keep the consistency of the BSSRDF, it also would result in very unintuitive editing operations, since volume properties are only very indirectly related to surface appearance. Additionally, direct observations of volumetric material properties is often not possible, necessitating complex indirect inference of the volumetric properties.

In this paper we propose *SubEdit*, a representation for editing measured heterogeneous subsurface scattering. The key to our representation is the decoupling of the effects of subsurface scattering between two surface locations as a product of two radial scattering profiles centered around the entry and exit points. Each profile captures the scattering behavior at a single surface location, and can be accurately approximated by a one-dimensional radial function. To provide an effective editing experience, we further reparameterize each scattering profile into the appearance concepts of albedo, scattering range, and profile shape. Furthermore, our representation makes selection more robust than when using the raw BSSRDF directly. The visual quality of the edited material is ensured by *SubEdit* since it automatically enforces the symmetry of subsurface light transport, it simplifies the enforcement of its decay with distance and it fits measured data well while remaining efficient enough to support interactive manipulations and rendering. Based on our representation users can perform complex editing operations with the same simplicity found in BRDF editing systems, while generating high quality non-local subsurface scattering effects (Figure 1).

In summary, as a representation for editing measured heterogeneous subsurface scattering, *SubEdit* has the following advantages:

- it decouples the non-local scattering effects of heterogeneous subsurface datasets into local scattering properties, simplifying editing and selection while ensuring visual quality;
- it allows the direct manipulation of intuitive aspects of the appearance of each surface location (albedo, scattering range and shape) to further simplify editing and to allow the straightforward definition of complex operations;
- it accurately fits measured datasets while allowing interactive editing and rendering.

## 2 Related Work

**BSSRDF Editing:** A number of methods have focused on editing homogeneous subsurface scattering materials [Xu et al. 2007; Wang et al. 2008b]. These methods are specifically tailored towards homogeneous subsurface scattering, and cannot be easily extended to handle heterogeneous subsurface scattering. In contrast, in this work we propose a method specifically designed for editing measured heterogeneous subsurface scattering materials.

Chen et al. [2004] proposed shell texture functions for modeling heterogeneous scattering materials based on shell volumes that are specified by user. While they are able to obtain good results, it is not clear how to create shell texture functions from measured heterogeneous materials. Wang et al. [2008a] developed a method, based on the diffusion equation, that can render and edit heterogeneous scattering materials interactively. Using an inverse rendering technique, relevant material properties can be extracted from measured heterogeneous scattering materials. Both methods rely on a volumetric representation. Obtaining a specific effect by editing such a volumetric representation is not always consistently effective

because of the complicated scattering behavior inside the volume (i.e., there is no direct mapping from editing operations to appearance properties of the material). The presented method on the other hand allows the user to directly control appearance properties of the scattering material: albedo, scattering range, and scattering profile.

**BSSRDF Representation:** Jensen et al. [2001] presented a practical dipole model to compactly represent homogeneous subsurface scattering materials. A number of researchers have extended this model to heterogeneous skin BSSRDFs by fitting dipoles for each surface point [Tariq et al. 2006; Donner et al. 2008] or per region [Weyrich et al. 2006; Ghosh et al. 2008]. While this representation is intuitive, it is limited to heterogeneous subsurface scattering materials with slowly varying material properties such as skin.

Tong et al. [2005] noted that a large class of materials falls in the category of quasi-homogeneous materials, i.e., locally heterogeneous but homogeneous at a larger scale. Their representation, however, cannot be easily extended to handle general heterogeneous subsurface scattering materials.

Lensch et al. [2003] and Goesele et al. [2004] decompose general BSSRDFs into a local and a global term. The local term represents the effects of incident illumination at a surface point in a local neighborhood. This is compactly represented by a filter kernel. The remaining long distance interactions are modeled by an approximate low resolution global term. Editing is difficult due to the tight coupling of the local and global term, and due to the non-parametric representation of the global term.

Fuchs et al. [2005] fit the BSSRDF at each point of a heterogeneous subsurface scattering material by a summation of radial exponential fall-off functions, and represent the spatial varying parameters in textures. Peers et al. [2006] use a data-driven representation for the average scattering function, and factorize spatial variations in terms of incident and outgoing locations via a modified non-negative matrix factorization. Both methods essentially encode heterogeneous subsurface scattering properties in a number of textures. It is not clear how these intertwined textures can be edited in a coherent and effective manner.

*SubEdit* differs from the above methods in that it is explicitly designed with editing in mind. In particular our representation decouples the BSSRDF in local scattering profiles, which further allows us to reparameterize the local scattering profiles into appearance concepts: albedo, scattering range, and scattering profile shape. Furthermore, with the prior representations it is not trivial to ensure that the edited material remains consistent. Our representation allows us to trivially maintain BSSRDF consistency.

## 3 Heterogenous Subsurface Scattering

**Background:** The behavior of subsurface scattering materials is described by the *bidirectional subsurface scattering distribution function* (BSSRDF)  $S(\mathbf{x}_i, \omega_i; \mathbf{x}_o, \omega_o)$  [Nicodemus et al. 1977] that relates the outgoing radiance  $L(\mathbf{x}_o, \omega_o)$  at a point  $\mathbf{x}_o$  in direction  $\omega_o$  to the incoming radiance  $L(\mathbf{x}_i, \omega_i)$  as

$$L(\mathbf{x}_o, \omega_o) = \int_A \int_{\Omega} S(\mathbf{x}_i, \omega_i; \mathbf{x}_o, \omega_o) L(\mathbf{x}_i, \omega_i) (\mathbf{n}(\mathbf{x}_i) \cdot \omega_i) d\omega_i d\mathbf{x}_i, \quad (1)$$

where  $A$  is the area around the point  $\mathbf{x}_o$  and  $\Omega$  is the hemisphere around  $\mathbf{x}_i$ , and  $\mathbf{n}(\mathbf{x}_i)$  is the surface normal at  $\mathbf{x}_i$ . The above equation can be separated into a local component, which accounts for light immediately reflected from a surface, and a global component, which captures the light scattering in the material volume. As in [Goesele et al. 2004; Peers et al. 2006], we focus our work on the

latter component that is captured by the so-called *diffuse BSSRDF*  $S_d$ , which we further decompose as

$$S_d(\mathbf{x}_i, \omega_i; \mathbf{x}_o, \omega_o) = \frac{1}{\pi} F_i(\mathbf{x}_i, \omega_i) R_d(\mathbf{x}_i, \mathbf{x}_o) F_o(\mathbf{x}_o, \omega_o), \quad (2)$$

where  $F_o$  and  $F_i$  are angular dependent functions, while  $R_d$  is a four dimensional function of two surface locations that encodes the spatial subsurface scattering of heterogeneous materials. Again following [Goesele et al. 2004; Peers et al. 2006], we focus exclusively on a representation for the 4D spatial component of the diffuse BSSRDF  $R_d$  and ignore the angular dependencies.

**Acquisition:** The BSSRDF of real material samples can be easily acquired by scanning each surface point with a light beam and recording the responses over the full surface [Goesele et al. 2004]. Depending on the scanning resolution, this process can be time consuming. Peers et al. [2006] sped up this process by scanning a flat sample surface with a regular grid of light beams (emitted from a projector) and captured several disjunct BSSRDF slices of illuminated grid surface points in each step which are separated during post-processing. In this paper, we follow the same approach for capturing the diffuse BSSRDF from flat material samples.

## 4 Representation

In this section, we present the *SubEdit* representation by first identifying the goals that a representation geared toward editing should fulfill. We then describe our model and show how it can be used to represent measured heterogeneous subsurface scattering. Finally, we briefly discuss its representational flexibility and limitations.

### 4.1 Goals

**Editability:** Our foremost consideration in the development of a representation suitable for editing is to simplify artistic exploration by providing direct controls to alter surface appearance. In the case of BSSRDFs, a representation should explicitly simplify three main aspects of the editing workflow. First, while the BSSRDF is a function defined over pairs of surface locations, it is often the case that the intent of the user is to alter the appearance at single surface points. The representation should facilitate such manipulation by allowing users to modify the scattering behavior at each point separately thus decoupling the non-local effects of subsurface scattering. Second, manipulation of the scattering behavior at each point should be intuitive by allowing users to manipulate parameters that are directly related to appearance. In the case of BSSRDFs, we believe that the user should be able to directly control surface albedo, its scattering range and, to a lesser extent, the shape of the decay. Finally, to facilitate editing of sets of surface points, the representation should facilitate the robust selection of surface locations of similar appearance. Supporting these three aspects will not only ensure quick direct manipulation, but will drastically simplify complex editing operations that can now be expressed trivially as combinations of these basic manipulations. An example of such complex edits are shown in Figure 1.

**Visual Quality:** Editing measured materials requires a careful balance between artistic control and the need for image quality. We need to ensure that the edited materials maintain their consistency, such that they exhibit no visual artifacts when rendered. In the case of BSSRDFs, we believe the following two properties should be maintained at all times to ensure visual quality. First, the diffuse BSSRDF is symmetric with respect to surface location, i.e.,  $R_d(\mathbf{x}_i, \mathbf{x}_o) = R_d(\mathbf{x}_o, \mathbf{x}_i)$ . Breaking this symmetry creates artifacts, shown in Figure 2, that are particularly visible under patterned lighting. Second, the BSSRDF at a point decays

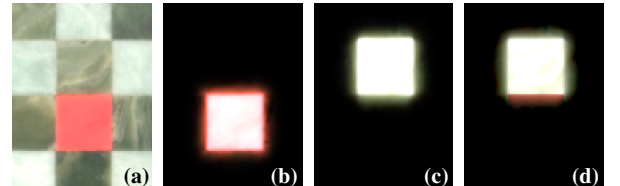


**Figure 2:** Importance of symmetry of scattering in BSSRDFs. (a) A checkerboard made of two translucent materials. The albedo of one white square is changed to red, without adjusting the properties of other squares. (b,c) The effect of illuminating two neighboring squares with a single beam of light covering exactly one square. Note that the color bleeding from the two regions is not consistent. (d) The correct color bleeding when enforcing symmetry of scattering in BSSRDFs.

with the distance from that point, i.e.,  $R_d(\mathbf{x}_i, \mathbf{x}_o) \leq R_d(\mathbf{x}_i, \mathbf{x}'_o)$  for  $|\mathbf{x}_i - \mathbf{x}'_o| > |\mathbf{x}_i - \mathbf{x}_o| + \delta$ . While heterogeneous BSSRDFs do not have a strong monotonicity guarantee, due to changes in the local physical properties of surrounding points, when looking at distances larger than some  $\delta$  a decay is observed. A representation suitable for editing should thus facilitate the enforcement of these two properties. Note that while we specifically choose not to enforce energy conservation to support artistic freedom, as in recent work on BRDF editing [Lawrence et al. 2006; Pellacini and Lawrence 2007], doing so would be straightforward in our representation.

**Accuracy:** Needless to say, our representation should accurately capture the intricate behavior of measured data, with a particular emphasis on spatially-varying heterogeneity of the BSSRDF. Equally important is that the representation should be powerful enough to support artistic freedom, such that it can represent the complex modifications an artist would like to apply to the surface appearance.

**Efficiency:** To provide a meaningful editing experience, the manipulation and rendering of the material should be interactive. The major roadblock in attaining interactivity is the huge data size of measured BSSRDFs, which necessitate compression to achieve interactivity. Although we seek good compaction of the measured data, it should not limit artistic exploration of the BSSRDF appearance. Thus we strive for interactivity while balancing compactness and editability.

### 4.2 SubEdit Representation

In developing our representation, we strive to support artistic exploration while maintaining visual quality. As discussed previously, the major roadblock we face is the non-local relations within the BSSRDF. This behavior makes editing cumbersome for users while complicating the enforcement of symmetry. To overcome these difficulties we propose to decouple the non-local behavior of the diffuse BSSRDF  $R_d$  as a product of local scattering profiles  $P_{\mathbf{x}}(\mathbf{d})$  defined at each surface location<sup>1</sup>  $\mathbf{x}$ , and parameterized over local position  $\mathbf{d} = \mathbf{x}_i - \mathbf{x}_o$ :

$$R_d(\mathbf{x}_i, \mathbf{x}_o) = \sqrt{P_{\mathbf{x}_i}(-\mathbf{d}) P_{\mathbf{x}_o}(\mathbf{d})}. \quad (3)$$

We chose this practical representation since it matches the behavior of light transport in the scattering medium. Intuitively, our representation can be seen as a decomposition of the diffuse BSSRDF

<sup>1</sup> The unspecified surface location  $\mathbf{x}$  is used to express that the particular equation in which it occurs holds for both the incident  $\mathbf{x}_i$  and outgoing  $\mathbf{x}_o$  surface locations. Note that  $P_{\mathbf{x}_i}$  and  $P_{\mathbf{x}_o}$  refer to the same function when  $\mathbf{x}_i = \mathbf{x}_o$ .

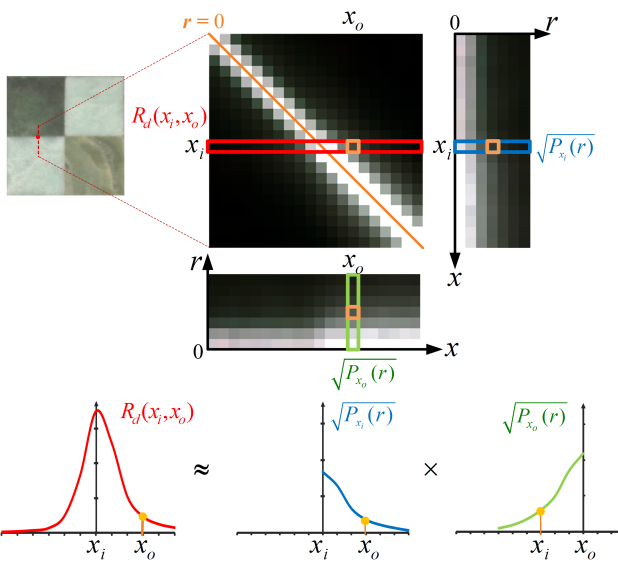


**Figure 3:** SubEdit representation illustrated on the scattering profiles along a line on a measured chessboard material. The subsurface transport from a single entry to exit point (marked in orange) is expressed as the product of corresponding points in the factored scattering profiles at  $\mathbf{x}_i$  (marked in blue) and at  $\mathbf{x}_o$  (marked in green).

in an entrance phase and an exitance phase. During the entrance phase an incident ray enters the material at  $\mathbf{x}_i$ , and travels some distance proportional to  $\|\mathbf{d}\|$  while being attenuated proportional to  $\mathbf{d}$ . Next, during the exitance phase, the ray scatters back toward the surface, again traveling a distance proportional to  $\|\mathbf{d}\|$  while being attenuated proportional to  $\mathbf{d}$ . The total effect of both attenuation events is the product of both.

The representation in Equation (3) still requires the same amount of storage as the diffuse BSSRDF  $R_d$ . As noted before, this large size is detrimental to interactivity. A crucial observation in reducing the storage requirements is that the scattering profiles  $P_x$  can be well approximated by radial scattering profiles represented by single 1D curves:

$$P_x(\mathbf{d}) \approx P_x(r), \quad (4)$$

with  $r = \|\mathbf{d}\| = \|\mathbf{x}_i - \mathbf{x}_o\|$ . To better model the exponential falloff displayed by the BSSRDFs and the scattering profiles of real materials (illustrated in Figure 4), we store the logarithm of the scattering profiles as a piecewise linear function of radius  $r$  with  $n$  segments as

$$\ln P_x(r) = \hat{P}_x(r) = (1 - w_x^k)\hat{P}_x^k + w_x^k\hat{P}_x^{k+1}, \quad (5)$$

for  $kr_s < rn \leq (k+1)r_s$ , and where  $r_s$  is the maximum scattering radius of the BSSRDF,  $\hat{P}_x^k$  is the value of the scattering profile at  $r_k = kr_s/n$  and  $w_x^k = rn/r_s - k$  is the linear weight for the  $k$ -th segment of the profile. Note that we only use this logarithmic representation  $\hat{P}_x(r)$  for efficient storage and data fitting (Section 4.3). All editing operations (Section 5) are defined on scattering profiles  $P_x(r)$ .

To gain some intuition on the relation between the BSSRDF and SubEdit profiles, we show each of them for a one dimensional slice of a measured chessboard dataset in Figure 3. Note that although each scattering profile is a smooth radial function, its shape can vary over the surface. Thus the heterogeneity of subsurface scattering is modeled by the product of spatially-varying 1D scattering profiles. Figure 4 shows the BSSRDFs, the scattering profiles, and the BSSRDF reconstructed for such profiles, for a few points of the

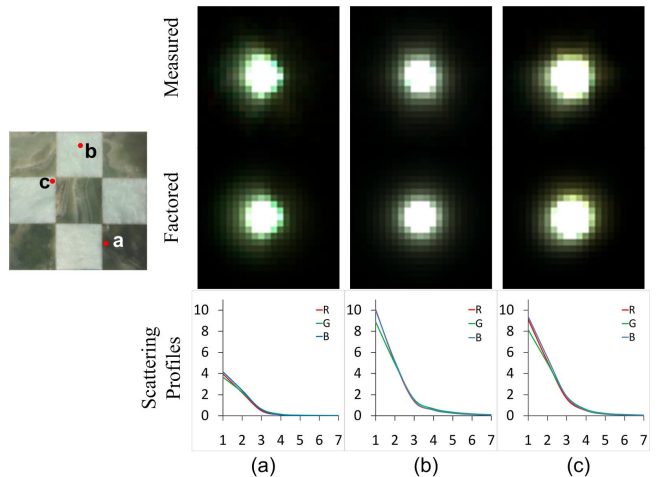


**Figure 4:** The measured BSSRDFs, factored BSSRDFs and the scattering profiles from three locations of a measured chessboard sample (left). Visual inspection of the measured and factored BSSRDFs suggest that our SubEdit representation fits measured data well. Furthermore, while the BSSRDF at locations (b,c) are different, their similar local material properties are captured by the similar SubEdit scattering profiles.

measured chessboard dataset. As is shown, the scattering profiles capture accurately the variations of the measured material BSSRDF.

In summary, SubEdit can be viewed as *decoupling the non-local scattering behavior of the BSSRDF into per-point scattering properties captured by the single scattering profiles*. This is one of the main advantages of our work over manipulating the BSSRDF directly. From a user interaction point of view, users can directly manipulate and select local scattering properties while our representation simplifies the enforcement of consistency properties. Symmetry, the most complex of them, is inherently maintained by the very form of the representation. Decay can be enforced by ensuring the monotonicity of the profiles themselves. Optionally, energy conservation can be enforced by bounding the integral over the scattering profiles to a maximum value.

### 4.3 Representing Measured Materials

**Algorithm:** To represent measured materials, we fit the logarithm of measured BSSRDF data

$$2 \ln(R_d(\mathbf{x}_i, \mathbf{x}_o)) = \ln P_{\mathbf{x}_o}(r) + \ln P_{\mathbf{x}_i}(r) = \hat{P}_{\mathbf{x}_i}(r) + \hat{P}_{\mathbf{x}_o}(r) \quad (6)$$

with the logarithm of the scattering profiles  $\hat{P}_x(r)$  by minimizing their  $L^2$  error over the object surface:

$$\int_{\mathbf{x}_o \in A} \int_{\mathbf{x}_i \in A} [2 \ln R_d(\mathbf{x}_i, \mathbf{x}_o) - (\hat{P}_{\mathbf{x}_i}(r) + \hat{P}_{\mathbf{x}_o}(r))]^2 d\mathbf{x}_i d\mathbf{x}_o. \quad (7)$$

For BSSRDF data measured over  $m$  discretized surface locations  $\mathbf{x}$ , minimizing this quadric function leads to a system of  $m^2$  linear equations with  $(n+1)m$  unknowns, one for each  $R_d(\mathbf{x}_i, \mathbf{x}_o)$ . This can be written as:

$$\begin{aligned} 2 \ln(R_d(\mathbf{x}_i, \mathbf{x}_o)) &= (1 - w_{\mathbf{x}_i}^k)\hat{P}_{\mathbf{x}_i}^k + w_{\mathbf{x}_i}^k\hat{P}_{\mathbf{x}_i}^{k+1} \\ &+ (1 - w_{\mathbf{x}_o}^k)\hat{P}_{\mathbf{x}_o}^k + w_{\mathbf{x}_o}^k\hat{P}_{\mathbf{x}_o}^{k+1}. \end{aligned} \quad (8)$$

We solve this large but sparse linear system using the conjugate gradient method [Press et al. 1992]. In practice, we found that this linear system is ill-conditioned, resulting in non-stable solutions that can yield non-monotonic scattering profiles. We therefore add a regularization term  $\lambda \int_{\mathbf{x}_i \in A} \int_r \nabla^2 \hat{P}_x(r) dr d\mathbf{x}_i$ , which ensures

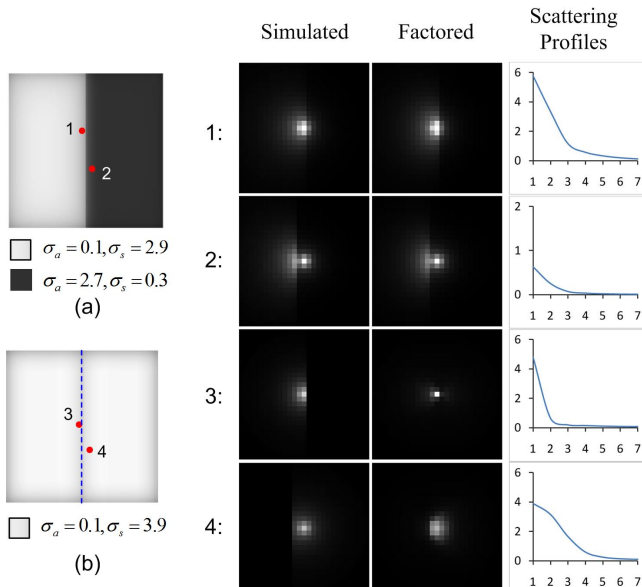


**Figure 5:** Simulated BSSRDF data, factored BSSRDFs and the scattering profiles from two locations of (a) a synthetic material volume that consists of two materials; (b) an extreme case where a synthetic homogeneous base material sample includes a narrow light blocking discontinuity marked in blue. The relevant material properties are denoted below each albedo map.

smoothness of the scattering profiles along the radius and adds the following  $(n - 1)m$  extra equations in the linear system:

$$\lambda [\hat{P}_{x_i}^k + \hat{P}_{x_i}^{k+2} - 2\hat{P}_{x_i}^{k+1}] = 0, \quad (9)$$

for:  $i = 0, 1, \dots, m - 1$ , and,  $k = 0, 1, \dots, n - 3$ . The regularization term, together with the original quasi-monotonic behavior of the measured BSSRDFs, effectively results in monotonic scattering profiles. For all results shown in this paper, we experimentally set  $\lambda = 0.01$ , and fit the BSSRDF data for each color channel separately.

**Discussion:** Our approach decouples the BSSRDF into a set of one-dimensional scattering profiles defined at each point. This decoupling drastically simplifies editing operations while maintaining the heterogeneity present in the measured data. As we will discuss in Section 7, our representation fits measured data well with a relative error comparable to prior work.

To validate the representational power of our representation, we performed a series of synthetic experiments on two synthetic  $64 \times 64 \times 32$  volumes with material properties varying along a single direction only. These datasets are the results of a photon mapping simulation. Each synthetic dataset is subsequently approximated by the proposed *SubEdit* representation. As illustrated in Figure 5 (a), our representation can model sharp discontinuities in material properties well, even if the fitted BSSRDF at each location is the product of two smooth scattering profiles. Our model captures these sharp discontinuities through the non-smooth variations of the scattering profiles between neighboring surface points.

The main limitation of our representation is that it can fail to reproduce strong anisotropic scattering behavior created by very narrow (i.e., less than the acquisition sampling rate) discontinuities in the material volume that completely block light transport between neighboring surface points with similar material properties. An example of such an extreme case is shown in Figure 5 (b). Nevertheless, despite this limitation, our representation can still represent a wide variety of measured materials in practice.

## 5 Subsurface Scattering Editing

Material editing is typically comprised of a selection operation followed by the manipulation of the appearance functions at the selected locations. In this section, we will show how *SubEdit* simplifies each of these aspects, selection and appearance manipulation, for datasets of measured heterogeneous subsurface scattering. Section 7 shows more complex edits made possible by *SubEdit*.

### 5.1 Scattering Profile Parameterization

Rather than editing the scattering profiles  $P_x$  directly, we propose to nonlinearly reparameterize these functions to allow the direct and independent manipulation of three basic properties of the underlying scattering behavior at a point  $x$ : its *diffuse albedo*  $C_x$ , its *scattering range*  $\alpha_x$ , and the *normalized shape* of the scattering profile  $S_x(r')$ . Using these quantities we can reparameterize the scattering profile as:

$$P_x(r) = \frac{C_x}{\alpha_x^2} S_x\left(\frac{r}{\alpha_x}\right). \quad (10)$$

The surface albedo, defined as  $C_x = \int_0^\infty P_x(r) r dr$ , captures the local color of the material. The scattering range captures the maximum radius at which the profile of a point has an appreciable effect. We define this quantity as the value  $\alpha_x$  for which  $P_x(r) < \varepsilon, \forall r \leq \alpha_x$ , with  $\varepsilon$  some small value (0.01% of the maximum of  $P_x$  in our implementation). The normalized scattering profile  $S_x$  captures the shape representing the effect of the chosen point's decay.  $S_x$  is a monotonic function defined in the  $[0, 1]$  interval such as  $\int_0^1 S_x(r) r dr = 1$ .

Figure 6 shows how by altering these three properties we obtain appearance modifications. Changing the albedo map directly maps to differences in the surface color. The scattering range controls the overall translucency of each point. When it is increased, the subsurface scattering from the selected points to surrounding regions is enhanced, giving the impression of a more translucent material and resulting in stronger back-lighting effects as well as a blurrier appearance of texture details. Conversely, when the scattering range is decreased, the extent of subsurface scattering shrinks to smaller regions, giving the impression of a more opaque material and resulting in a sharper look to texture details and a reduced effect of back-lighting. Finally, the normalized shape of a scattering profile changes the gradient of subsurface scattering decay around the selected surface points, leading to variations in the contrast of the texture details within the scattering range. Compared to manipulations of albedo or scattering range, the visual impact of changes to scattering shape is the most subtle.

The above parameterization of the scattering profiles in components that directly map to appearance concepts is an integral part of what makes *SubEdit* an effective representation for editing. We believe this to support intuitive editing for three reasons. First, it allows users to directly access to these quantities and easily manipulate the corresponding scattering behaviors, rather than requiring modifications of free-form curves. Second, these quantities are independent thus allowing even quicker control since changes to one are visually independent from the others, e.g., albedo and scattering range. Third, operations that would be remarkably complex to perform on the raw BSSRDF data or even on the original profiles can now be described as a collection of simple operations defined over these parameters. Figure 1 and Section 7 demonstrate such edits. Finally, interpolation of these quantities is well defined, as we will describe in the next paragraphs. This allows us to implement painting and filtering tools inspired by Photoshop or perform edit propagation as in [Pellacini and Lawrence 2007]. In a way, this parameterization brings the same simplicity and level of control typically found in

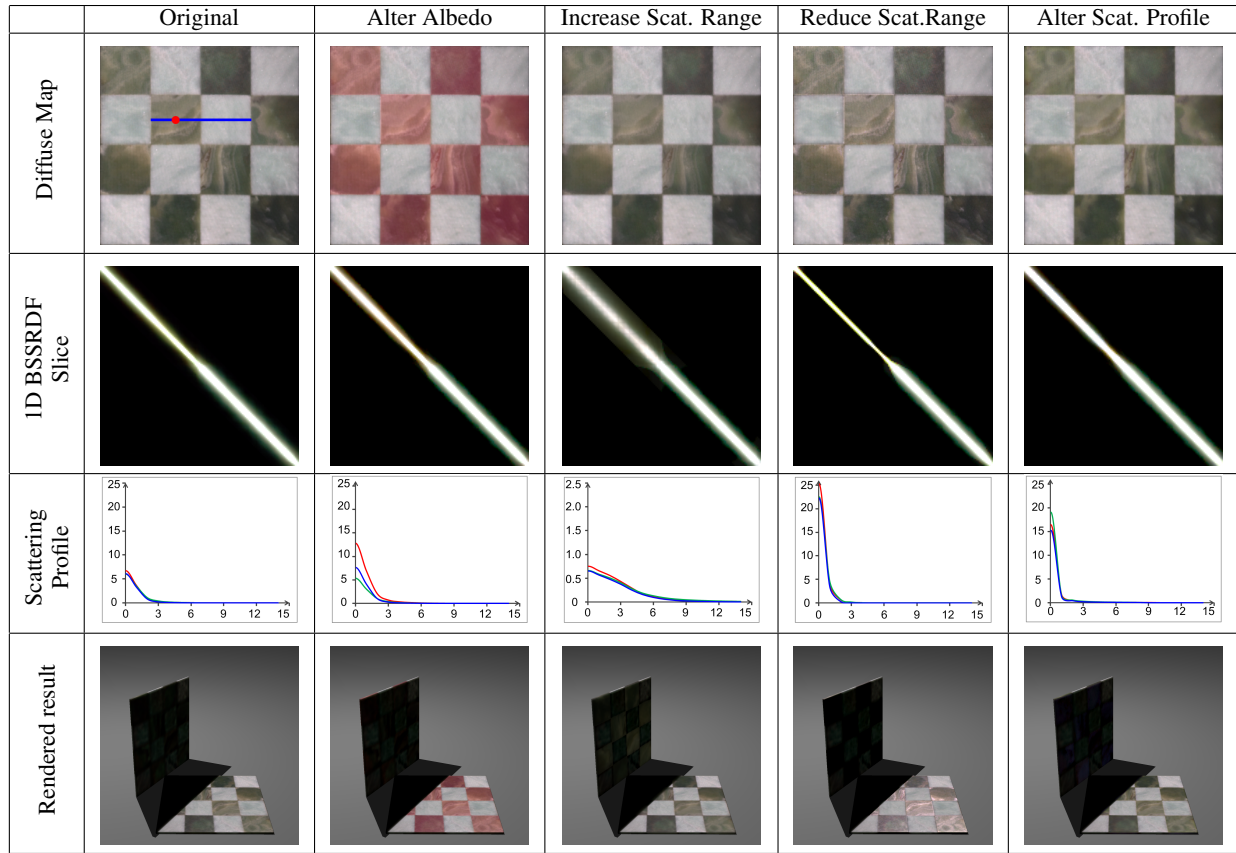


**Figure 6:** Illustration of changing different SubEdit properties: albedo, scattering range, and scattering profile shape. The first row shows the diffuse map of materials under uniform lighting. The second row shows a 1D slice of the BSSRDF (marked in blue). The scattering profile of the red marked point is shown in the third row. The last row shows the rendering results of the altered materials.

editing analytic BRDF models for the manipulation of measured heterogeneous subsurface scattering.

## 5.2 Edit Propagation

In this work we propose to edit the spatially-varying properties at selected surface points by using an appearance-driven optimization, where a user scribbles on different parts of the surface and those scribbles are subsequently propagated to all points in the dataset [Lischinski et al. 2006; Pellacini and Lawrence 2007; An and Pellacini 2008] to compute soft selection masks that are then used to linearly interpolate editing parameters defined at each stroke. Figure 6 uses edit propagation to alter only the green squares of the checkerboard.

**Soft Selection:** While different propagation algorithms have been proposed, they all rely on the definition of a metric that computes the pairwise distances  $d$  between the appearance of two points on the surface  $\mathbf{x}$  and  $\mathbf{y}$ . While one could choose to compute an appearance metric by computing the  $L^2$  distance of the raw BSSRDFs (i.e.,  $d_b^2(\mathbf{x}, \mathbf{y}) = \int_{\mathbf{x}'} ||R_d(\mathbf{x}, \mathbf{x} + \mathbf{x}') - R_d(\mathbf{y}, \mathbf{y} + \mathbf{x}')||^2 d\mathbf{x}'$ ), we argue that such a choice would not be intuitive to edit with. The reason behind this is that the BSSRDF at a point can be affected by other points on the surface, thus making it hard to separate different materials that might be present on the surface. Figure 7 shows an example of this behavior on a selection performed in a measured artificial stone made of three distinct materials. Note how using a raw BSSRDF distance metric yields a selection that includes both background and blue particle regions, even though the underlying

materials in the selected regions are distinctly different. This is a direct consequence of the non-local scattering behavior of BSSRDFs.

Using SubEdit, one can define the distance between the appearance of two points by computing the distance between the scattering profiles at each location written as

$$d^2(\mathbf{x}, \mathbf{y}) = \int_0^\infty \|P_\mathbf{x}(r) - P_\mathbf{y}(r)\|^2 r dr. \quad (11)$$

As shown in Figure 7, this distance metric better captures the structure of the underlying material and provides better results that include blue particles only since our representation factors the BSSRDF into the local appearance of each surface point, by explicitly expressing the BSSRDF in terms of an incident term and an exitant term. In our prototype implementation we opted to pair our metric with AppWand [Pellacini and Lawrence 2007] as the selection algorithm, since it was specifically designed for materials. However, any other region-based selection tool can also be used.

**Edit Interpolation:** The selection mechanism listed above requires edits to single locations to be propagated to all other points by linear interpolation of editing parameters. Our parameterization allows us to simply interpolate scale and offsets values for edits to albedo and scattering range, following recent work on BRDFs [Pellacini and Lawrence 2007]. Note that performing similar edits on the BSSRDF itself would require complex non-linear optimization to impose the edit while maintaining visual quality. Finally, propagating edits to the scattering shape is slightly more complex since we allow users to perform unrestricted manipulations in the editing user interface, while at the same time we want to ensure the monotonicity and normalization of the resulting shape func-

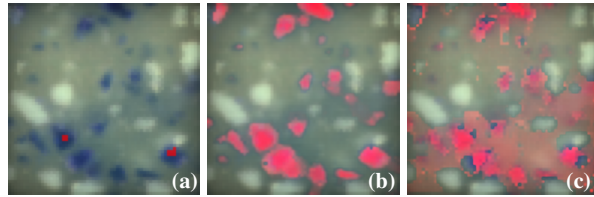


**Figure 7:** Comparison of selection directly on the raw BSSRDF and on the scattering profiles. (a) the diffuse albedo of the artificial stone material with the selected points marked in red. (b) the selection based on the scattering profiles, and (c) the selection based on the raw BSSRDF. The former is able to distinguish better between the different materials, and yields a more intuitive selection result.

tions. In our implementation we simply propagate scale and offsets at each sample along  $r$  and alter the functions accordingly. After propagation, we impose monotonicity by ensuring that  $\hat{P}_x^{k+1} > \hat{P}_x^k$  and renormalize the functions themselves. A result of edit interpolation is illustrated in Figure 9(b), where a small white region is selected, and its scattering range is reduced by the user. This editing operation is then smoothly propagated to all regions of similar appearance using edit interpolation. After editing, the shadow of the elephant’s trunk becomes harder due to the reduced scattering range. Note how the translucency of the blue wax looks natural after editing while maintaining the progressive variations exhibited in the original material.

## 6 Interactive Editing Visualization

An integral part of material editing is to provide real-time feedback of the edited appearance over arbitrary geometry. While efficient rendering is not the focus of our work, we implemented a simple GPU renderer in our prototype editor to interactively render the edited results in this paper. We visualize the edited subsurface scattering effects on different geometries by applying the material to the vertices of sufficiently-tessellated meshes by the two pass method of Jensen and Buhler [2002]. In the first pass, we sample the irradiance on each mesh vertex, based on shadow map visibility for directional or point lighting, or from pre-computed radiance transfer techniques for environmental illumination [Ng et al. 2003; Wang et al. 2008b]. In the second pass, we compute the outgoing radiance of each vertex by integrating the contributions from all surrounding surface vertices using Equation (1), where the BSSRDF  $R_d$  between two vertices is evaluated by the scattering profiles of two vertices. We use an octree of vertices to restrict this integration to the spatial neighbors of each vertices that fall in the scattering range and parallelize this computation on a GPU using CUDA. For directional or point light sources, we also add the contribution of specular reflectance.

## 7 Results

We tested our representation by implementing a prototype editing system running on a PC with 3.20GHz Pentium 4 CPU with 1.5GB RAM and an NVIDIA GeForce 8800 GTX video card with 768MB video memory. All images were rendered with our interactive renderer at 0.5 – 2 frames per second.

**Measured Materials:** We evaluated our representation with a set of measured materials with different kinds of heterogeneity, shown in Figure 8. Table 1 lists statistics of the measured BSSRDF datasets and their scattering profile factorizations. We fit the measured data with our model using 24 segments for  $\hat{P}_x$ , achieving a good balance between data size and accuracy; in fact, further in-

Sample Material	Resolution (pixels)	Fitting (Min.)	Orig. Size	SubEdit Size	Min/Aver/Max Relative Error
Chessboard	222 × 222	25.3	674	13.5	0.009/0.067/0.169
Blue Wax	88 × 232	10.3	286	5.6	0.004/0.031/0.095
Artif. Stone	108 × 108	5.7	163	3.2	0.003/0.029/0.098
Jade	260 × 260	34.0	947	18.6	0.008/0.062/0.158
Yellow Wax	110 × 110	6.0	169	3.3	0.004/0.023/0.075

**Table 1:** Statistics of the measured BSSRDFs and the fitted scattering profiles of the heterogeneous subsurface scattering materials shown in Figure 8.

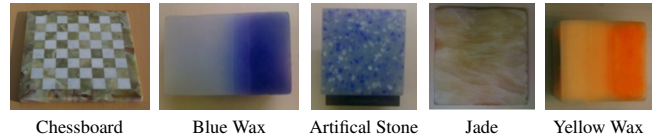


**Figure 8:** The photographs of measured BSSRDF samples.

creasing the number of segments does not significantly improve the fit. Fitting takes between 10 and 30 minutes for datasets ranging from roughly 200 MB to 1 GB. Following [Peers et al. 2006], we measure the quality of the fit by computing the minimum, average and maximum of the relative errors at each surface location between the measured data and the reconstructed data normalized by the total energy of the response. As illustrated in Table 1, the error statistics show that our representation has overall data sizes similar (3 – 19 MB) compared to the results of [Peers et al. 2006], while allowing editing, albeit at a slightly larger relative error (2 – 7%). Also note that while *SubEdit* is less suited for representing highly anisotropic scattering behavior, it is still capable of representing the anisotropic jade material, albeit at a slightly lower accuracy.

### 7.1 Complex Edits

The decoupling of subsurface appearance into local scattering profiles, together with the reparameterization presented previously, allows us to quickly implement complex edits to measured subsurface scattering datasets. These operations would be nearly impossible to perform using the BSSRDF itself. The following presents a few examples of such operations to demonstrate *SubEdit*, but we expect artists to be able to perform a large class of additional operations with the same ease. With our prototype implementation, a user can generate each of the editing results shown in the paper in between 10 and 20 minutes.

**Pattern Copy-Paste:** In many circumstances it is desirable to extract interesting material variations from one region or a different material and apply it to the current selection. We therefore define a copy-paste operator that first extracts the desired patterns, and subsequently transfers it to the target. To extract the pattern over varying scattering profiles, we first compute the gradient of scattering profile  $\hat{P} = (\hat{C}, \hat{\alpha})$  by applying a standard gradient operator on both albedo and scattering range. To apply the extracted pattern to a new region, we compute the new scattering profile at each point by solving the Poisson equation as in [Gangnet and Blake 2003] for albedo and scattering range. The profile shape is kept unchanged in this operation. A result of this operator is shown in Figure 1(c) where the chessboard pattern is transferred onto the yellow wax and mapped onto the Buddha model. Note that both the variations in the chessboard and the appearance of yellow wax material are maintained in the edited BSSRDF. A second example is shown in Figure 9(c) where a pattern is extracted from a user specified image and then pasted on the elephant’s body.

**Material Painting:** A common editing requirement is to create a mixture of some component from two datasets or from two different

surface points. This can be obtained in a straightforward manner by linearly blending the albedo, range and shape of the profiles. Formally, the linear blending of two properties can be computed as  $\kappa'(\cdot) = w\kappa_s(\cdot) + (1-w)\kappa_d(\cdot)$ , where  $w$  is the blending weight specified by the user, and  $\kappa(\cdot)$  can be any scattering profile property ( $C$ ,  $\alpha$ , or  $S$ ).

An application of such a blending operation is material painting, where the source scattering profile is specified by the user or selected from a surface point, and the destination scattering profiles are the selected target surface points. A first example is shown in Figure 1(b), where a complex interpolation, following the underlying geometrical structure, of the yellow and blue wax materials is shown. The interface between both materials is automatically dealt with by our representation. A second example of material blending can be seen in Figure 10(b) where the jade material is blended with the yellow wax progressively varying from top left to bottom right. Figure 10(c) illustrates another example, where the albedo of the jade is kept unchanged, while its scattering range and shape are replaced with the scattering range and shape of the white marble in the chessboard dataset. After editing, the blended material maintains the texture variations in the original material but exhibits less translucency.

**Material Filtering:** *SubEdit* factors the BSSRDF in a two dimensional collection of scattering profiles. Consequently, many image filtering operations can also be applied directly to manipulate the albedo, scattering range and shape of the profiles. Figure 11 illustrates several material editing results generated by filtering the artificial stone material. Using a bilateral filter on the albedo and scattering range on a selected region, i.e., the white and blue stones, we can create the appearance of moving the stones deeper inside the material volume (Figure 11 (b)). Conversely, applying an unsharp mask on the albedo and scattering ranges of the white stones increases the apparent difference in subsurface scattering compared to the blue stones, making them appear closer to the surface (Figure 11 (c)). Furthermore, we set the filter kernel as roughly the size of the individual stones. Due to the decoupling and intuitive reparameterization of the BSSRDF, *SubEdit* can generate complex editing results using well-known image filter operations.

**BSSRDF Hallucination:** As a final example of a complex editing operation, we create the hallucination of a completely new BSSRDF from a single photograph under fixed lighting of a translucent material sample plus a different measured BSSRDF dataset. This is obviously an ill-defined problem, and an exact recreation of the BSSRDF of the material in the photograph is not possible. However, it is still possible to create a plausible BSSRDF that would correspond to the photograph. This can then be directly used for rendering, or serve as a basis for further edits. To this end, the user first copies scattering profiles from one or more measured BSSRDFs and assigns these to a few representative surface points in the photograph. Next, the scattering range and shape of the assigned scattering profiles are propagated to all other surface points. We use *AppWand* [Pellacini and Lawrence 2007] for propagation where the distance between two pixels is computed as the  $L^2$  distance of the pixel values in the Lab color space. The color value at each pixel is used as the albedo of result scattering profiles. Additional control on the propagated profiles can be achieved by providing a different guidance image, instead of the *albedo* image, to propagate the scattering profiles.

Figure 1(d) shows an example of BSSRDF hallucination. Here we used *only* a photograph of the target red-and-yellow wax material from [Peers et al. 2006], and marked a few corresponding scattering functions on the source yellow-wax shown in Figure 1(a), and propagated these to the remaining surface points. Additionally, we also reduced the scattering ranges on the target red wax to better match

the original material. The resulting visualization of the hallucinated BSSRDF is a plausible reconstruction and artifact free. Note that both scattering range and albedo vary in the resulting BSSRDF. This cannot be achieved by a homogeneous BSSRDF modulated by the input texture image only. Figure 12 shows three additional BSSRDF hallucinations. For each material the original photograph is shown in the inset. The scattering profiles used for three results are picked from measured stone, jade and marble datasets respectively.

## 8 Conclusions and Future Work

In this paper we presented *SubEdit*, a representation for editing measured heterogeneous subsurface scattering. Our representation makes artistic modifications efficient and at the same time ensures good visual quality. The key of our method is the decoupling of the non-local scattering properties into per point radial scattering profiles. This decoupling allows users to directly modify the scattering of single surface locations and makes selection robust. Furthermore, thanks to this decoupling, *SubEdit* ensures the visual quality and the consistency of edited BSSRDFs by automatically enforcing the symmetry of subsurface light transport as well as simplifying enforcement of its decay with distance. To further enhance the editing experience, we reparameterize each scattering profile into albedo, scattering range and profile shape, quantities that directly map to appearance concepts. Finally, we showed how our representation fits measured data well while remaining efficient for interactive visualization. All of these properties combined allow us to quickly perform complex editing operations on measured heterogeneous materials.

In the future we are interested in expanding the range of complex editing operations based on *SubEdit*. We also would also to investigate the use of a perceptual metrics and reparametrizations for even more intuitive editing and selection of the scattering profiles. Finally, we are interested in exploring rendering algorithms to employ *SubEdit* directly in realtime applications.

## Acknowledgements

The authors would like to thank Yang Zhang for the implementation of the fitting algorithm, Qiang Dai for assisting in raw data capture, Jiaping Wang for discussions on BSSRDF fitting and decomposition, Matthew Callcut and Bruce Lamond for proofreading the paper, and Matthew Callcut for dubbing the video. The authors also thank JiaoYing Shi, Baining Guo, Saskia Mordijk, Monica Nichelson, Paul Debevec, Bill Swartout, Randy Hill, and Randolph Hall for their generous support to this project. Finally, we thank the anonymous reviewers for their helpful suggestions and comments. Fabio Pellacini was supported by NSF (CNS-070820, CCF-0746117) and Intel Corporation. Pieter Peers was supported by the U.S. Army Research, Development, and Engineering Command (RDECOM) and the University of Southern California Office of the Provost. The content of the information does not necessarily reflect the position or the policy of the U.S. Government, and no official endorsement should be inferred.

## References

- AN, X., AND PELLACINI, F. 2008. AppProp: all-pairs appearance-space edit propagation. *ACM Trans. Graph.*, Vol. 27, No. 3, 40:1–40:10.



**Figure 9:** An elephant visualized with the blue wax dataset. (a) The original material. (b) The scattering range is reduced for the light colored wax. (c) A pattern pasted on the body.



**Figure 10:** Statue rendered with the jade dataset. (a) The original material. (b) A new material obtained by gradually blending the jade material with the yellow wax material. (c) A new material obtained by blending the scattering range and profile shape of jade with those of the white marble of the chessboard dataset.



**Figure 11:** The dragon rendered with the artificial stone dataset. (a) The original material. (b) Bilateral filtering applied to the blue and white stones only. (c) Unsharpening applied to the blue and white stones.

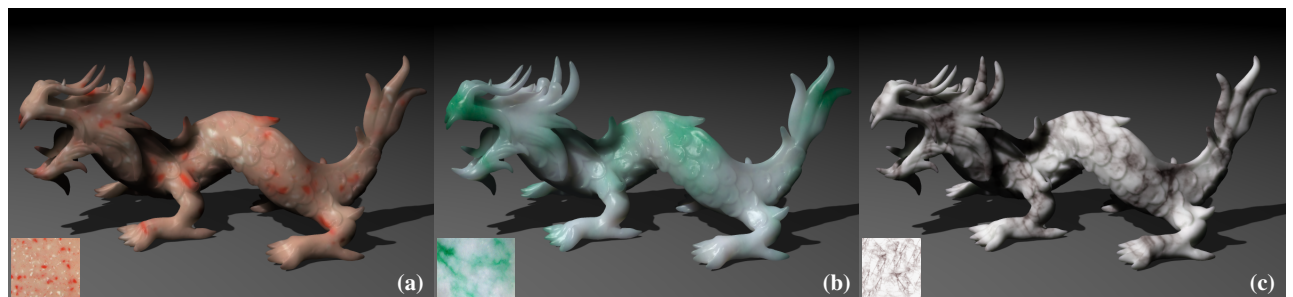


**Figure 12:** The Asian dragon model visualized with hallucinated BSSRDFs. The source images used to hallucinate from are shown in the insets. (a) A red stone material hallucinated from the artificial stone material. (b) A green jade material generated from the jade dataset. (c) A marble BSSRDF hallucinated from the chessboard dataset.

- CHEN, Y., TONG, X., WANG, J., LIN, S., GUO, B., AND SHUM, H.-Y. 2004. Shell texture functions. *ACM Trans. Graph.*, Vol. 23, No. 3, 343–353.
- DONNER, C., WEYRICH, T., D'EON, E., RAMAMOORTHI, R., AND RUSINKIEWICZ, S. 2008. A Layered, Heterogeneous Reflectance Model for Acquiring and Rendering Human Skin. *ACM Trans. Graph.*, Vol. 27, No. 5, 140.
- FUCHS, C., GOESELE, M., CHEN, T., AND SEIDEL, H.-P. 2005. An Empirical Model for Heterogeneous Translucent Objects. In *ACM SIGGRAPH Sketches*.
- GANGNET, M., AND BLAKE, A. 2003. Poisson image editing. *ACM Trans. Graph.*, Vol. 22, No. 3, 313–318.
- GHOSH, A., HAWKINS, T., PEERS, P., FREDERIKSEN, S., AND DEBEVEC, P. 2008. Practical Modeling and Acquisition of Layered Facial Reflectance. *ACM Trans. Graph.*, Vol. 27, No. 5, 139.
- GOESELE, M., LENSCHE, H. P. A., LANG, J., FUCHS, C., AND SEIDEL, H.-P. 2004. DISCO: acquisition of translucent objects. *ACM Trans. Graph.*, Vol. 23, No. 3, 835–844.
- JENSEN, H. W., AND BUHLER, J. 2002. A rapid hierarchical rendering technique for translucent materials. *ACM Trans. Graph.*, Vol. 21, No. 3, 576–581.
- JENSEN, H. W., MARSCHNER, S. R., LEVOY, M., AND HANRAHAN, P. 2001. A practical model for subsurface light transport. In *Proc. ACM SIGGRAPH*, 511–518.
- LAWRENCE, J., BEN-ARTZI, A., DECORO, C., MATUSIK, W., PFISTER, H., RAMAMOORTHI, R., AND RUSINKIEWICZ, S. 2006. Inverse Shade Trees for Non-Parametric Material Representation and Editing. *ACM Trans. Graph.*, Vol. 25, No. 3.
- LENSCHE, H. P. A., GOESELE, M., BEKAERT, P., MAGNOR, J. K. M. A., LANG, J., AND SEIDEL, H.-P. 2003. Interactive Rendering of Translucent Objects. *Computer Graphics Forum*, Vol. 22, No. 2, 195–205.
- LISCHINSKI, D., FARBMAN, Z., UYTENDAELE, M., AND SZELISKI, R. 2006. Interactive local adjustment of tonal values. In *ACM Trans. Graph.*, 646–653.
- NG, R., RAMAMOORTHI, R., AND HANRAHAN, P. 2003. All-frequency shadows using non-linear wavelet lighting approximation. *ACM Trans. Graph.*, Vol. 22, No. 3, 376–381.
- NICODEMUS, F. E., RICHMOND, J. C., HSIA, J. J., GINSBERG, I. W., AND LIMPERIS, T. 1977. *Geometrical Considerations and Nomenclature for Reflectance*. National Bureau of Standards (US).
- PEERS, P., VOM BERGE, K., MATUSIK, W., RAMAMOORTHI, R., LAWRENCE, J., RUSINKIEWICZ, S., AND DUTRÉ, P. 2006. A compact factored representation of heterogeneous subsurface scattering. *ACM Trans. Graph.*, Vol. 25, No. 3, 746–753.
- PELLACINI, F., AND LAWRENCE, J. 2007. AppWand: editing measured materials using appearance-driven optimization. *ACM Trans. Graph.*, Vol. 26, No. 3, 54.
- PRESS, W. H., ET AL. 1992. Numerical Recipes in C (Second Edition). *Cambridge University Press*.
- TARIQ, S., GARDNER, A., LLAMAS, I., JONES, A., DEBEVEC, P., AND TURK, G. 2006. Efficiently Estimation of Spatially Varying Subsurface Scattering Parameters. In *11th Int'l Fall Workshop on Vision, Modeling, and Visualization 2006*, 165–174.
- TONG, X., WANG, J., LIN, S., GUO, B., AND SHUM, H.-Y. 2005. Modeling and rendering of quasi-homogeneous materials. *ACM Trans. Graph.*, Vol. 24, No. 3, 1054–1061.
- WANG, R., TRAN, J., AND LUEBKE, D. 2005. All-Frequency Interactive Relighting of Translucent Objects with Single and Multiple Scattering. *ACM Trans. Graph.*, Vol. 24, No. 3, 1202–1207.
- WANG, J., ZHAO, S., TONG, X., LIN, S., LIN, Z., DONG, Y., GUO, B., AND SHUM, H.-Y. 2008. Modeling and rendering of heterogeneous translucent materials using the diffusion equation. *ACM Trans. Graph.*, Vol. 27, No. 1, 9:1–9:18.
- WANG, R., CHESLACK-POSTAVA, E., LUEBKE, D., CHEN, Q., HUA, W., PENG, Q., AND BAO, H. 2008. Real-time editing and relighting of homogeneous translucent materials. *The Visual Computer*, Vol. 24, 565–575(11).
- WEYRICH, T., MATUSIK, W., PFISTER, H., BICKEL, B., DONNER, C., TU, C., MCANDLESS, J., LEE, J., NGAN, A., JENSEN, H. W., AND GROSS, M. 2006. Analysis of human faces using a measurement-based skin reflectance model. *ACM Trans. Graph.*, Vol. 25, No. 3, 1013–1024.
- XU, K., GAO, Y., LI, Y., JU, T., AND HU, S.-M. 2007. Real-time homogenous translucent material editing. *Computer Graphics Forum*, Vol. 26, No. 3, 545–552.